Mo-Sleep: Unobtrusive Sleep and Movement Monitoring via Wi-Fi Signal

Fan Li*, Cheng Xu*, Yang Liu†, Yun Zhang*, Zhuo Li*, Kashif Sharif *, Yu Wang‡
* School of Computer Science, Beijing Institute of Technology, China
† School of Automation, Beijing Institute of Technology, China
‡ Department of Computer Science, University of North Carolina at Charlotte, USA

***Abstract*—Sleep monitoring system helps to diagnose various health problems. Traditional solutions for sleep monitoring are usually invasive or limited to medical facilities. Radio Frequency (RF) based methods require specialized devices or dedicated wireless sensors. Recently, Wi-Fi based methods without any wearable or dedicated devices obtain more attention, however, they all assume that all the users are in a relatively quiet environment without moving targets. In this paper, we develop a system called Mo-Sleep, which adopts off-the-shelf Wi-Fi devices to continuously collect fine-grained wireless Channel State Information (CSI) in a room. We introduce a motion detection module in our system to identify whether the CSI information has been interfered by a moving target. We then use Principal Component Analysis (PCA) to obtain accurate breath signal. Our prototypic system demonstrates that the proposed scheme can not only remove interfered CSI, but also obtain real time breath rate every five seconds.**

I. Introduction

Sleep is one of the most familiar activities in our daily life. About one third of the time in our lives is occupied by sleep. When falling asleep, individual brain and body can have a good rest, however, with the development of society, some people suffer from insomnia due to high pressure. Poor sleep often leads to some diseases, such as diabetes, obesity and depression [1]. Although a lot of people are suffering from these sleep problems, few people can properly evaluate their sleep quality. Currently, there are many commercial sleep monitoring systems in the market [2]–[4], but most of these applications and systems force users to wear extra devices, such as wristband or headset. Data collected from these extra devices can be used to infer and analyze sleep quality directly or indirectly. However, these extra devices are obtrusive and uncomfortable for users to wear. Besides, many sleep monitoring systems can only provide coarse-grained sleeping information (for example, total sleep time) [5].

In order to improve the precision of sleep monitoring, some non-obtrusive systems have been proposed recently. Most of them take advantage of pressure sensor arrays embedded in blanket or mattress to monitor sleep, by providing fine-grained sleep information, such as breath rate and heart rate. However, it is too costly for people to afford. At the same time, while visual and acoustic signal are also exploited to realize sleep monitoring, they are not only vulnerable to illumination intensity, but also cause serious privacy problems [6], [7]. Recently, a sleep monitoring system, called iSleep, is developed to monitor sleep based on microphone embedded in smart phone [8]. However, this method is very sensitive to environment noise, thus impractical for real world implementation.

To address those limitations mentioned above, sleep monitoring systems based on RF (Radio Frequency) have attracted much attention due to its non obtrusiveness. Doppler radar [9] and WiSpiro [10] are used to capture person's breath information, however, they are expensive and require complicated devices, which are not suitable for long-term and stable monitoring. Wi-Sleep [11] and Tracking Vital Signal [12] take advantage of off-the-shelf Wi-Fi devices to provide fine-grained breath information which are non-obtrusive, low cost, and easy to implement, however, they can only work in a quiet environment. When people walking around the monitored user, it will have great impact on the measured results. The waveform of CSI subcarriers changes up-and-down with the movement of chest. When someone moves around, the waveform of the subcarriers can no longer accurately reflect people's breath. In order to deal with this problem, we design a motion detection module, which makes a judgement whether there are moving targets around the users.

CSI can provide fine-grained amplitude and phase information of multiple OFDM (Orthogonal Frequency Division Multiples) subcarriers. For example, current mainstream Wi-Fi systems, like 802.11 a/g/n, are based on OFDM containing 52 subcarriers. Because of the the frequency diversity, multiple effects and shadow fading, the amplitude of these subcarriers might have significant changes, thus the movement in physical environment would cause the change of subcarriers' amplitude. Due to the fact that the moving targets have a significant impact on the amplitude of subcarriers, subcarriers amplitude can no longer reflect the breath accurately, even the person is in a normal breath status. As a result, previous sleep monitoring systems might get a wrong result if there are moving targets, such as moving people, pets, sliding door and windows. In our work, Mo-Sleep takes advantage of off-the-shelf Wi-Fi devices to catch vital breath movement, meanwhile to remove the interfered CSI when we detect that there are moving targets. The main contributions of our work are summarized as follows.

- We use Principal Component Analysis (PCA) to remove noise from the signals by taking advantage of the correlated variations in CSI of different subcarriers. PCA can reduce the scale of data at the same time preserve original principal information, thus we do not have to

design a subcarriers selection strategy to select the best subcarrier.

- We introduce a motion detection module into our system. Through the CSI data collected by off-the-shelf Wi-Fi devices, we can determine whether there is a moving target around the user. The accurate breath signal can be obtained by removing interfered CSI.
- Compared with other sleep monitoring systems, our system can provide real time breath signal and breath rate every 5 seconds.

The rest of the paper is organized as follows. Section II gives an overview of the system architecture. In Section III, we present a brief introduction of the background of CSI, and carry out outlier removing. After that, we introduce breath monitoring module and motion detection module in Section IV and Section V, respectively. In Section VI, we present the experiment settings and demonstrate the results. Finally, the related works are discussed in Section VII, and a brief conclusion is provided in Section VIII.

II. System Overview

We use the CSI in physical layer as the initial indicator. The rationality of our monitoring work is that some of the propagation paths can be disturbed by even very small movements. This type of disturbance can be recorded by the temporary changes of CSI and reflected in the CSI time series. As shown in Figure 1, the system takes raw CSI data as the input, which can be collected through off-the-shelf Wi-Fi devices when people are sleeping. In order to achieve respiratory detection, we divide the system into two modules: *breath monitoring module*, and *motion detection module*. Raw CSI data may contain many outliers, we use outliers filter to remove them before breath monitoring and motion detection. Breathing is a type of low frequency movement, therefore the respiratory monitoring module aims to filter the coming data by low pass filter to remove the high frequency components of the data. After that, we use PCA to reduce data dimension as well as eliminate noise further. After we obtain the breath signal, we determine the user's breath rate by calculating the distance between the peaks of the signal.

Additionally, raw CSI data contains significant phase random noise, thus we adopt phase calibration in the motion detection module. Feature extraction part is the core of the motion detection module. In order to avoid the influence of different transmitting power in a specific scenario, we choose the eigenvalues of the correlation coefficient matrix of CSI amplitude and phase values in a time window. In this paper, we choose decision tree classifier to judge whether there is a moving object according to the eigenvalues.

In the end, we combine the results of the motion detection module and the breath monitoring module to make final judgment. If there are moving targets infect the breath signal, the motion detection module can detect it and the system will output nothing, otherwise, the system will output the detected breath rate.

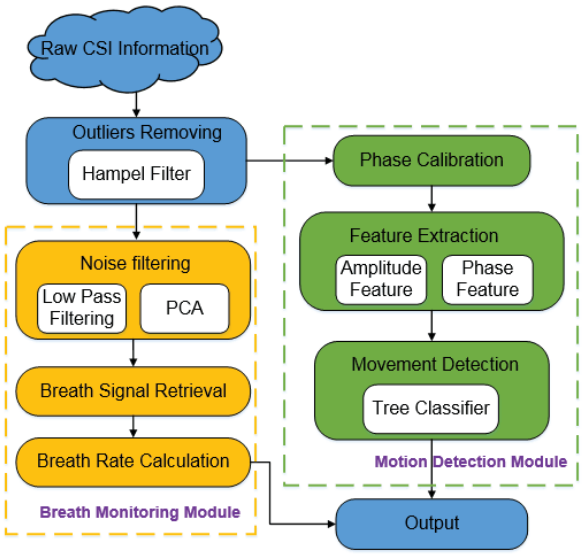

Figure 1. The overview of our sleep monitoring system, Mo-Sleep.

III. Preprocessing

With the development of OFDM technology, subcarrier level channel measurement becomes feasible. CSI is used to evaluate the channel quality of communication links. More specifically, CSI describes a process in which signal propagates from the transmitter to the receiver, and can reflect the combined effect of distance, scattering, decline, and power attenuation in the process of transmission. In general, the CSI measurement precision is good enough to reflect the channel state information of system based on OFDM. In a narrow flat fading channel, OFDM system is modeled in frequency as:

$$y = Hx + N, \tag{1}$$

where x and y represent the transmitter vector and receiver vector respectively , H represents the channel state matrix, and N is an additive white gaussian noise. For a single subcarrier, it can be denoted in a mathematical form as

$$h = |h|e^{j \sin \theta}, \tag{2}$$

where $|h|$ and θ denote the amplitude and phase of each subcarrier respectively [13]. By modifying the firmware, normal Wi-Fi devices can obtain the sampling of 30 subcarriers. So in one data packet, the CSI can be expressed as

$$H = [h_1, h_2, h_3 \ldots, h_n], \tag{3}$$

where n is the number of subcarriers, and we set $n = 30$ in this paper.

A. Outlier Removing

From Figure 2, we observe that raw CSI contains many outliers, which are generated from protocol specifications as well as environment noise. Breath is one type of low frequency movement, thus these outliers can affect our breath monitoring and motion detection. The first step is of Mo-Sleep is to use

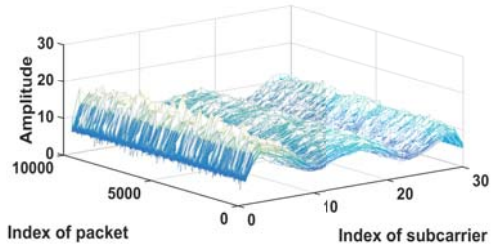

(a) 3D raw CSI time series

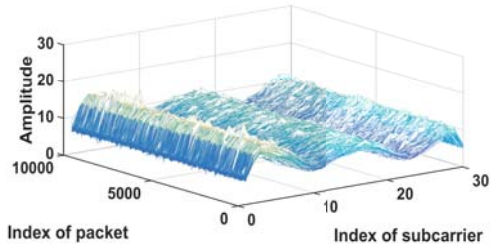

(b) 3D CSI time series after outlier removing

Figure 2. The amplitude of 3D raw CSI time series before and after applying outlier removing.

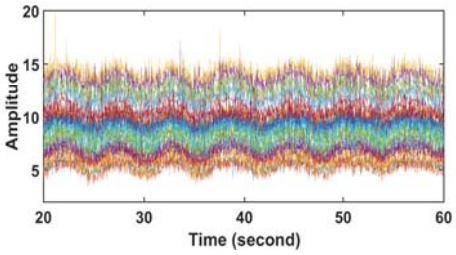

(a) 2D CSI time series

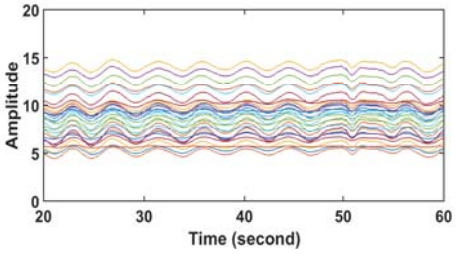

(b) 2D CSI time series after passing low pass filtering

Figure 3. The amplitude of 2D CSI time series before and after passing low pass filtering.

Hampel identifier [14] to remove outliers. Hampel identifier declares that any point falling out of the closed interval $[\mu - \gamma\sigma, \mu + \gamma\sigma]$ is an outlier, where μ and σ are the median and the Median Absolute Deviation (MAD) of the data sequence, respectively. γ is an application dependent parameter and the most widely used value is 3. Figure 2 (b) shows the result of outlier removing. Window size is set to 100 and $\gamma = 3$.

IV. Breath Monitoring Module

Breath monitoring module contains noise filtering, breath signal retrieval and breath rate calculation, which are introduced below respectively.

A. Noise Filtering

The CSI we collected from commodity Wi-Fi NICs contains all kinds of noise. Before we recognize breath signal from CSI, such noise need to be removed from CSI. Firstly, we pass the CSI from a low pass filter to remove high frequency noises. However, a simple low pass filter cannot remove the noise efficiently, because the low frequency part also contains noise. In order to extract useful information from noisy CSI, we leverage the observation that the variation in the CSI of all subcarriers due to the chest are correlated. Consequently, we apply Principal Component Analysis (PCA) on the filtered subcarriers to extract the signals caused only contain the variation only caused by the movement of chest. Below, we first introduce the process of applying low pass filter to remove high frequency, then we explain how to extract breath signals with our PCA based method.

1) Low Pass Filtering: Generally speaking, the respiratory frequency of an adult is between 10 to 14 breathes per minute (bpm) [15], a newly born baby's respiratory frequency is faster, which is about 37 bpm [16]. Thus we set the range of normal respiratory frequency as 10 to 37 bpm, and the estimated normal respiratory frequency is in the range of 0.17-0.62 Hz. According to the above analysis, frequency changes caused by breath happens in the low frequency domain of the spectrum, whereas the noise generally occupies the whole frequency range. In our work, we employ Butterworth low pass filter to filter every subcarrier wave. Compared with other filters, Butterworth filter has a maximum flat amplitude response in the pass band. From Figure 3, we observe that while the high-frequency noise is filtered by Butterworth filter commendably, noise is not completely eliminated, because the Butterworth filter has slightly slow fall off in the stopband. In the following, we employ PCA to further filter CSI time series.

2) PCA Based Filtering: PCA cannot only reduce the dimension of high-dimensional data, but also find the pattern of data as well as achieve noise removing. In Figure 3(b), quite similar variations of waveform are illustrated between adjacent subcarriers, however, non-adjacent subcarriers which are far away in frequency do not show such similar variation of their waveforms. Although without similar changes, these subcarriers are still correlated to some extent. We take advantage of the correlation between subcarriers to calculate principal component from all CSI subcarriers. The derived principal components represent the most common variation in all subcarriers.

The reasons we employ PCA is that PCA can decrease the scale of data at the same time preserve original principal information. PCA can reduce the dimension of data as well as replace n features of original samples with m fewer newer features without information loss. The new features are the linear combination of old features, which maximize sample variance and try to make m new features uncorrelated with

each other. Mapping old features to new features enables us to capture intrinsic variation of data. Decreasing scale of data contributes to reduce computation complexity as well as improving system response time which is very important to breath monitoring. PCA can automatically provide us with breath signal, so there is no need to design a subcarrier selection strategy to choose the best signal to represent breath movement. PCA helps to remove some uncorrelated noise components which cannot be filtered by traditional low pass filter from the filtered data by taking advantage of correlated variations in CSI subcarriers.

B. Breath Signal Retrieval

We use HP_i to denote the time series of the ith subcarrier after low-pass filter. HP_i is a $m \times 1$ vector, where m is the total number of collected packets. HP is a $m \times n$ vector, where n is the total number of subcarriers, so we have

$$HP = [HP_1, HP_2, HP_3, ..., HP_n], \tag{4}$$

where the ith column denotes the time series of the ith subcarrier. Next we show how PCA works:

1) Normalizing HP. We normalize the HP matrix such that each CSI time series has zero mean and unit variance. We use $\overline{HP}$ to represent the normalized version of HP. The normalization means each element of the column in HP subtracts the mean value of the column, consequently, the mean value of each column in $\overline{HP}$ is 0.

2) Calculating the covariance matrix of $\overline{HP}$. S is used to denote the covariance matrix of $\overline{HP}$, it is a $m \times n$ matrix. Φ_S is a $n \times n$ dimensional matrix, which is made up of EigenVectors of S. We denote $\Phi_S^{\{1:p\}}$ as the top p principal components obtained from PCA in $\overline{HP}$. We set p to 2 in our work. The reason is that we observe in our experiment that the top two principal components can almost contain 98% information of $\overline{HP}$ as shown in Figure 4.

3) Obtaining the principal breath information from HP, we have

$$newHP = \overline{HP} \times \Phi_S^{\{1:2\}} \tag{5}$$

where $newHP$ is an $m \times 2$ matrix which contains the projected CSI information in its columns.

After having $newHP$, we calculate the breath signal as:

$$breathSignal = newHP^{\{1\}} \times \alpha + newHP^{\{2\}} \times \beta \tag{6}$$

where α and β are the weighted coefficients. Through extensive experiments, we found that when $\alpha = \beta = \frac{1}{2}$, our breath signal matches the ground truth in Figure 5. In this work, the ground truth refer to the moments we record with stopwatch when people take breath. Note that we record one time stamp when user's chest goes down to the lowest position, thus this time stamp corresponds to a peak in breath signal shown in Figure 5. The ground truth is shown as Table I.

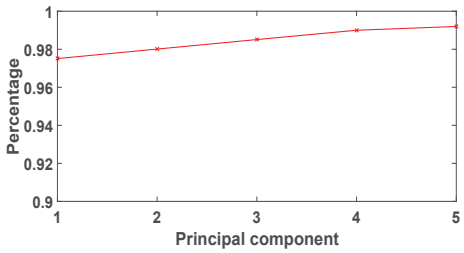

Figure 4. The top 5 principle components.

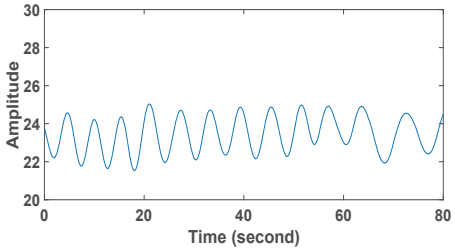

Figure 5. The breath signal obtained from $newHP$.

C. Breath Rate Calculation

We still want to get a simple value which denotes the breath rate of people sometimes. Consequently, we calculate the breath rate in this part. As shown in Figure 5, we estimate the breath rate by the peak-to-peak intervals. We collect peaks from the breath signal, then the peak-to-peak intervals can be represented as $P = [p_1, p_2, p_3, ..., p_u]$, where P is a vector which contains all the peak-to-peak intervals we collected in 20 seconds. We obtain total u peak-to-peak intervals from this $20s$ time window. E is breath cycle which can be calculated by $\arg_E \min \sum_{i=1}^{u} |E - p_i|^2$. Thus, we can obtain breath rate as:

$$R = \frac{60}{\arg_E \min \sum_{i=1}^{u} |E - p_i|^2}. \tag{7}$$

V. Motion Detection Module

Currently, the exiting work in breath monitoring focuses on quiet environment, which is impractical even in the bedroom. Sometimes people or other moving targets enter bedroom which results in the misjudgement for the breath status. As show in Figure 6, normal breath of person is affected by an adjacent moving target, resulting in subcarrier waveform distortion, so it is difficult to judge the person's breath status. In this paper, we propose to detect breath and the moving

Table I
Ground Truth Data

ith peaks	1	2	3	4	5	6
Time stamp (s)	4.7	10.1	15.5	21.1	27.3	33.4
ith peaks	7	8	9	10	11	12
Time stamp (s)	39.3	45.6	51.5	56.9	63.8	73.0

objects. In recent years, the intrusion detection and the passive detection of moving objects based on Wi-Fi have made great progress, and the precision has reached a relatively high level [17], [18]. In this paper, we extract the phase and amplitude information to judge whether there exists moving target. Beside fast-moving objects, this method is also sensitive to slow-moving objects with high accuracy. This module contains phase calibration, feature extraction and movement detection, which will be introduced respectively in this section.

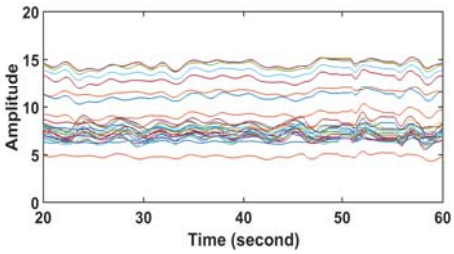

Figure 6. CSI time series influenced by a moving target.

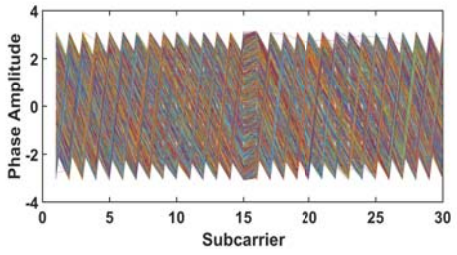

(a) Raw phase

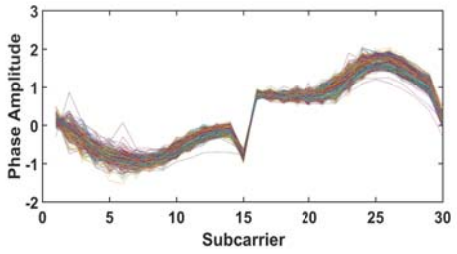

(b) Phase after calibration

Figure 7. Phase amplitude of 30 subcarriers before and after calibration.

A. Phase Calibration

Despite CSI is widely used in various applications, most applications take advantage of its amplitude features, the phase characteristics of CSI do not receive enough attention. The main reason is that it is difficult to obtain reliable phase information in the existing commercial equipments. Due to the randomness of noise which is caused by reflections, diffractions, refractions and asynchronism of transceiver, the original phase information might induce random phase offset.

We remove the random phase offset from the original phase by mathematical linear transformation. More specifically, the ith measured subcarrier phase information can be expressed as follows:

$$\hat{\phi}_i = \phi_i - 2\pi \frac{K_i}{B}\delta + \beta + Z, \tag{8}$$

where ϕ_i represents the true phase, δ denotes the time offset at the receiving end, β is the unknown phase deviation, and Z is a measurement noise. K_i is the index value of ith subcarrier. According to the IEEE 802.11n standard, the index value is: -28, -26, -24, -22, -20, -18, -16, -14, -12, -10, -8, -6, -4, -2, 1, 1, 3, 5, 7, 9, 11, 13, 15, 17, 19, 21, 23, 25, 27, 28. B is the size of the FFT, which is 64 according to the IEEE 802.11 a/g/n standard. Because of the uncertain phase information listed above, it is impossible to obtain the real phase information by using a commercial wireless card.

In order to reduce the influence of random noise, according to Equation 8, we process the original phase information using linear transformation proposed by PADS [18]. From Figure 7(b) we can see that phase after calibration presents more stable than the original one. The processed phase information cannot be regarded as a real one, but we obtain an effective form of real phase.

B. Feature Extraction

In previous work, a variety of statistical properties have been explored, such as mean [19], variance [20] and skewness [21]. All these statistics are based on amplitude information. Amplitude is related to the signal energy, which is sensitive to environmental temperature, humidity, and the device itself. Additionally, we know that phase information is more sensitive to slow motions [18], therefore, different from the previous work, we extract features from phase for motion detection. A lot of work has confirmed that people's movement lead to the change of amplitude and phase, but unfortunately, this change cannot be used as a feature directly because it is related to absolute energy, consequently, sensitive to different scenarios and equipments. As discussed above, different subcarriers show different correlations. In general, adjacent subcarriers have higher correlation, motion subcarriers have higher correlations than static subcarriers. So we assume that compared with the breath movement, subcarriers have stronger correlations when moving targets exist. We extract features from the normalized correlation coefficient matrix of the amplitude and phase respectively. If there is a vector $X = [X_1, X_2, X_3, \ldots, X_k]$, we define the correlation coefficient matrix as below:

$$\rho_{k\times k} = (\rho_{i,j} \quad \rho_{i,j} = \rho(\bar{X}_i, \bar{X}_j)), \tag{9}$$

where $\rho_{i,j}$ denotes the correlation coefficient between vector $\bar{X}_i$ and $\bar{X}_j$ and the $\bar{X}$ denotes the normalized X. CSI are continuously collected k measurements within a specific window from CSI time series which can be denoted as $\mathrm{H} = [H_1, H_2, H_3, \ldots, H_k]$. The k measurements of CSI are used as the input for our movement detection.

1) Amplitude Features: According to what we have discussed above, we extract amplitude feature from k measure-

ments, so we have

$$\rho_A = \begin{pmatrix} \rho(\bar{H}_1, \bar{H}_1) & \rho(\bar{H}_1, \bar{H}_2) & \cdots & \rho(\bar{H}_1, \bar{H}_k) \\ \rho(\bar{H}_2, \bar{H}_1) & \rho(\bar{H}_2, \bar{H}_2) & \cdots & \rho(\bar{H}_2, \bar{H}_k) \\ \vdots & & \ddots & \\ \rho(\bar{H}_k, \bar{H}_1) & \rho(\bar{H}_k, \bar{H}_2) & & \rho(\bar{H}_k, \bar{H}_k) \end{pmatrix}_{k \times k}, \quad (10)$$

where $\bar{H}_i$ denotes the standardized H_i. Generally speaking, higher correlation coefficient is more likely to link to moving targets presence scenario. In contrast, lower correlation coefficient is more likely to link to static scenario. We calculate the eigenvalues of correlation coefficient matrix and apply the maximum value as our amplitude features, i.e.,

$$a = \max(eigen(\rho_A)), \quad (11)$$

2) Phase Features: We use the same steps to process phase data. The phase correlation coefficient matrix in the sliding window is given as

$$\rho_P = \begin{pmatrix} \rho(\bar{\phi}_1, \bar{\phi}_1) & \rho(\bar{\phi}_1, \bar{\phi}_2) & \cdots & \rho(\bar{\phi}_1, \bar{\phi}_k) \\ \rho(\bar{\phi}_2, \bar{\phi}_1) & \rho(\bar{\phi}_2, \bar{\phi}_2) & \cdots & \rho(\bar{\phi}_2, \bar{\phi}_k) \\ \vdots & & \ddots & \\ \rho(\bar{\phi}_k, \bar{\phi}_1) & \rho(\bar{\phi}_k, \bar{\phi}_2) & & \rho(\bar{\phi}_k, \bar{\phi}_k) \end{pmatrix}_{k \times k}, \quad (12)$$

and the features extracted from phase are

$$c = \max(eigen(\rho_P)). \quad (13)$$

Finally, we obtain a two dimensional vector $Fea = [a, c]$. In order to guarantee the accuracy of detection, we introduce the second and third maximum eigenvalues of amplitude and phase respectively and thus devise a 6-tuple feature $Fea = [a1, a2, a3, c1, c2, c3]$, where $a1$, $a2$, $a3$ and $c1$, $c2$, $c3$ are the maximum, second maximum and third maximum eigenvalue for amplitude and phase respectively.

C. Motion Detection

As mentioned above, the performance of CSI-based motion detection highly depends on static multipath profile. That is to say, we need to retrain the classifier if we move the Wi-Fi device to another room. But we do not need to retrain the classifier with different moving targets. In particular, we propose a decision tree classifier to identify moving targets.

The decision tree is derived from the training data. The decision tree represents the decision set of a tree structure. It is made up of decision nodes, branches and leaves. The top of the nodes in the decision tree is the root node, each branch is a new decision node or the leaves of the tree. Each decision node represents a problem or decision, which usually corresponds to the properties of the classified object. Each leaf represents a possible classification result. Along the decision tree, each node will have a test. Each node will choose different branches according to different test outputs of the problem, and eventually reach a leaf node.

We collect sample data in our experiments for binary classification based on decision tree, to determine whether there is a moving object around. Our experiments validate the great performance of our methods in various moving objects, with different moving velocities. One of the most important reason is that the features we choose are independent on power fluctuation.

VI. Experiment Results

We evaluate out system in two aspects: (1) the capability to track the breath of a user with fixed sleeping position, and (2) the capability to detect motion.

The experimental environment is shown in Figure 8, which is in a meeting room about $5ft \times 6ft$. The distance between transmitter and receiver is set to $3m$. The transmitter broadcasts package to receiver every 20ms. We employ 5 students with different genders, heights, weights as our participants.

Figure 8. Experiment setup using CSI.

A. Tracking Respiration with Fixed Sleeping Positions

Each participant except participant 5 sleeps with normal breath rate for about 10 minutes. At the same time, the participant 5 sit $2m$ away from every participant to record his/her breath with a stopwatch, which is the ground truth of his/her breath status.

First, we evaluate the performance of our breath monitoring module. We set the sliding window size to be $20s$, and the window slides once every 5 seconds. If we collect data in t seconds, there are total k windows, where $k = t/5 - 1$. We calculate the breath rate in each sliding window. Let R be the breath rate we obtain from sliding window, R_g be the ground truth breath rate we calculate from the data recorded by stopwatch. We assume that if $|\mathrm{R} - \mathrm{R}_g| < 0.3\mathrm{bpm}$, the result is "Positive", otherwise, the result is "Negative". If there are total l "Positive" windows, the "Positive" rate can be denoted as

$$\mathrm{p}^+ = l/k. \quad (14)$$

Figure 9 shows that "Positive" rate is around 84% -96%, and the mean "Positive" rate is 90.75%, which demonstrates that our system can monitor users' breath with high accuracy.

B. Impact of Multiple Antennas

We explore multiple antennas to improve the precision and robustness of breath monitoring module. In the experiment, we use JHR-N835R router as the transmitter, which has three antennas. On the other hand, our receiver has two antennas. As

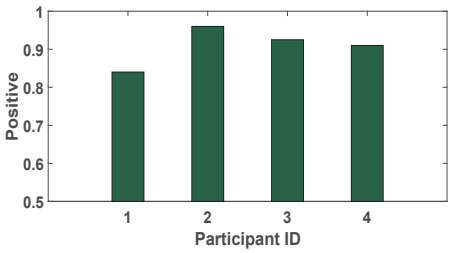

Figure 9. "Positive" rate by different participants.

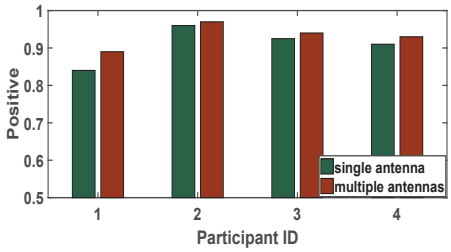

Figure 10. "Positive" rate with multiple antennas.

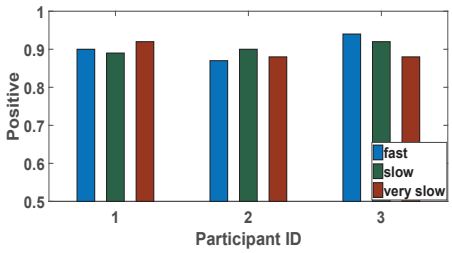

(a) Every participant walks with different velocity

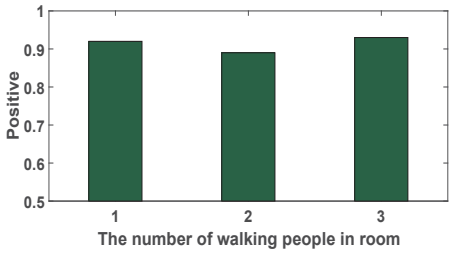

(b) Different number of participants walk in room

Figure 11. "Positive" rate with different moving patterns.

a result, we obtain six breath signals, we take the average for all the six breath signals. As shown in Figure 10, the precision of breath rate is better than the one with single antenna, and the mean precision is 93.5%.

C. Identifying Motion

When Participant 4 is sleeping, we ask another participant to walk in the room with different velocities (fast, slow ,very slow) for about 5 minutes respectively. In other two situations, we ask two and three participants walk in the room with with random velocities for about 5 minutes.

Figure 11 shows that our motion detection module is sensitive to various moving velocities and multiple persons. We can see from Figure 11(a) that our module can detect the moving people with average 90% no matter what kind of velocities they move. Figure 11(b) illustrates that our motion detection module works well in single person scenario as well as multiple persons scenario.

VII. Related Works

We summarize the related work into two parts: work related to sleep monitoring and work related to movement detection.

A. Sleep Monitoring

We all know that Photoplethysmography (PPG) [22] can provide useful information about individual's sleep, however, it is obtrusive for patients because their fingers have to be attached with some annoying sensors. To overcome this problem, plenty of less obtrusive or unobtrusive systems have been developed. For example, people need to wear some wrist bands [3], or probes [23] to continuously collect data from their body to infer the sleep condition. What's more, some totally unobtrusive systems also have been emerged recently. isleep [8] obtains sleep information from built-in microphone and smartphone. Whereas, this system is very sensitive to environment noise. Some other systems use specially designed blanket or belt put on bed to monitor people's sleep quality [24], [25].

Sleep monitoring systems based on RF (Radio Frequency) have attracted much attention due to its unobtrusiveness. Wi-Sleep [11] and Tracking Vital Signal [12] take advantages of off-the-shelf Wi-Fi devices to provide fine-grained breath information which are unobtrusive, low cost, and easy to implement. However, they can only work in a quiet environment. When people walking around the monitored user, it will have a great impact on the measured results. The waveform of CSI subcarriers changes up-and-down with the movement of chest. When someone moving around, the waveform of the subcarriers can no longer accurately reflect peoples breath.

B. Movement Detection

Device-free movement detection or localization gain more and more attention in recent years [26], [27]. Most CSI based work leverages the variations of CSI data to analyze target location or movements. Pilot [28] leverages the correlation of CSI time series in localization to monitor the presence of object then locate the object. Omnidirectional PHD [17] takes advantage of multipath effects of CSI to explore the Omnidirectional sensing of coverage of human detection. FCC [29] explores the crowd counting by analyzing the relationship between CSI variations and the number of people. PADS [18] leverages both amplitude and phase information from CSI to judge the presence of moving target.

VIII. Conclusions

In this paper, we propose to use commodity Wi-Fi devices to track user's breath status. In order to deal with unquiet

environment, we design a motion detection module to detect whether there are some moving targets interfering CSI time series. We apply PCA to obtain breath signal without designing subcarriers selection strategy. Our prototypic sleep and movement monitoring system demonstrates that it can obtain real time breath rate every five second. For future work, we intend to monitor the breath of multiple people simultaneously, and identify multiple movements like getting-up and hand movement.

ACKNOWLEDGMENT

The work is partially supported by the National Natural Science Foundation of China under Grant No. 61370192, 61432015, 61428203, 61572347, and 61602038, the China Postdoctoral Science Foundation under Grant 2015M580051 and Grant 2016T90039, and the US National Science Foundation under Grant No. CNS-1319915 and CNS-1343355.

REFERENCES

[1] J. Dostal, P. O. Kristensson, and A. Quigley, "Estimating and using absolute and relative viewing distance in interactive systems," *Pervasive and Mobile Computing*, vol. 10, pp. 173–186, 2014.
[2] Jawbone up. http://www.toodaylab.com/44685/.
[3] Fitbit. http://www.fitbit.com/.
[4] J. R. Shambroom, S. E. Fábregas, and J. Johnstone, "Validation of an automated wireless system to monitor sleep in healthy adults," *Journal of sleep research*, vol. 21, no. 2, pp. 221–230, 2012.
[5] Sleep cycle. http://www.pingwest.com/demo/sleep-cycle-alarm-clock/.
[6] W.-H. Liao and C.-M. Yang, "Video-based activity and movement pattern analysis in overnight sleep studies," in *19th International Conference on Pattern Recognition*, ICPR 2008, pp. 1–4, IEEE, 2008.
[7] Philips vital signs camera. http://www.vitalsignscamera.com/.
[8] T. Hao, G. Xing, and G. Zhou, "iSleep: Unobtrusive sleep quality monitoring using smartphones," in *ACM Conference on Embedded Networked Sensor Systems*, pp. 1–14, 2013.
[9] K. M. Chen, D. Misra, H. Wang, H. R. Chuang, and E. Postow, "An X-band microwave life-detection system," *IEEE Transactions on Biomedical Engineering*, vol. 33, no. 7, pp. 697–701, 1986.
[10] P. Nguyen, X. Zhang, A. Halbower, and T. Vu, "Continuous and fine-grained breathing volume monitoring from afar using wireless signals," in *The 35th Annual IEEE International Conference on Computer Communications*, IEEE INFOCOM, 2016.
[11] X. Liu, J. Cao, S. Tang, and J. Wen, "Wi-sleep: Contactless sleep monitoring via wifi signals," in *IEEE Real-time Systems Symposium*, pp. 346–355, 2014.
[12] J. Liu, Y. Wang, Y. Chen, J. Yang, X. Chen, and J. Cheng, "Tracking vital signs during sleep leveraging off-the-shelf WiFi," in *the 16th ACM International Symposium on Mobile Ad Hoc Networking and Computing*, pp. 267–276, 2015.
[13] K. Wu, J. Xiao, Y. Yi, M. Gao, and L. M. Ni, "Fila: Fine-grained indoor localization," in *the Annual IEEE International Conference on Computer Communications*, IEEE INFOCOM, vol. 131, no. 5, pp. 2210–2218, 2012.
[14] L. Davies and U. Gather, "The identification of multiple outliers," *Journal of the American Statistical Association*, vol. 88, no. 423, pp. 782–792, 1993.
[15] P. Sebel, *Respiration, the breath of life*. Torstar Books, 1985.
[16] P. C. Gay, "The normal lung: the basis for diagnosis and treatment of pulmonary disease," *Mayo Clinic Proceedings*, vol. 61, no. 7, p. 606, 1986.
[17] Z. Zhou, Z. Yang, C. Wu, L. Shangguan, and Y. Liu, "Towards omni-directional passive human detection," in *the Annual IEEE International Conference on Computer Communications*, IEEE INFOCOM, vol. 12, no. 11, pp. 3057–3065, 2013.
[18] K. Qian, C. Wu, Z. Yang, Y. Liu, and Z. Zhou, "Pads: Passive detection of moving targets with dynamic speed using PHY layer information," in *20th IEEE International Conference on Parallel and Distributed Systems (ICPADS)*, pp. 1–8, 2014.
[19] J. Wilson and N. Patwari, "Radio tomographic imaging with wireless networks," *IEEE Transactions on Mobile Computing*, vol. 9, no. 5, pp. 621–632, 2010.
[20] J. Wilson and N. Patwari, "See-through walls: Motion tracking using variance-based radio tomography networks," *IEEE Transactions on Mobile Computing*, vol. 10, no. 5, pp. 612–621, 2010.
[21] Y. Zeng, P. H. Pathak, and P. Mohapatra, "Analyzing shopper's behavior through WiFi signals," in *the 2nd workshop on Workshop on Physical Analytics*, pp. 13–18, 2015.
[22] N. H. Shariati and E. Zahedi, "Comparison of selected parametric models for analysis of the photoplethysmographic signal," in *International Conference on Computers, Communications, Signal Processing with Special Track on Biomedical Engineering*, pp. 169 – 172, 2005.
[23] J. Zhang, D. Chen, J. Zhao, and M. He, "Rass: A portable real-time automatic sleep scoring system," vol. 8537, no. 11, pp. 105–114, 2012.
[24] J. Paalasmaa, M. Waris, H. Toivonen, L. Leppakorpi, and M. Partinen, "Unobtrusive online monitoring of sleep at home," in *International Conference of the IEEE Engineering in Medicine Biology Society*, pp. 3784–8, 2012.
[25] Tanita. http://www.tanita.co.jp/products/models/s1501.html/.
[26] M. Youssef, M. Mah, and A. Agrawala, "Challenges: Device-free passive localization for wireless environments," in *International Conference on Mobile Computing and Networking*, ACM MOBICOM, pp. 222–229, 2007.
[27] L. Chang, X. Chen, Y. Wang, D. Fang, J. Wang, T. Xing, and Z. Tang, "FitLoc: Fine-grained and low-cost device-free localization for multiple targets over various areas," in *IEEE 35th Conference on Computer Communications*, IEEE INFOCOM, 2016.
[28] J. Xiao, K. Wu, Y. Yi, L. Wang, and L. M. Ni, "Pilot: Passive device-free indoor localization using channel state information," in *IEEE International Conference on Distributed Computing Systems*, pp. 236–245, 2013.
[29] W. Xi, J. Zhao, X. Y. Li, and K. Zhao, "Electronic frog eye: Counting crowd using wifi," in *IEEE Conference on Computer Communications*, IEEE INFOCOM, pp. 361–369, 2014.